HMG Advance Access published December 15, 2013

Human Molecular Genetics, 2013 **1–15**
doi:10.1093/hmg/ddt595

Calcium binding is essential for plastin 3 function in Smn-deficient motoneurons

Alison N. Lyon[1], Ricardo H. Pineda[1], Ie Thi Hao[1], Elena Kudryashova[2], Dmitri S. Kudryashov[2] and Christine E. Beattie[1,*]

[1]Department of Neuroscience, The Ohio State University, 132 Rightmire Hall, 1060 Carmack Rd, Columbus, OH 43210, USA and [2]Department of Chemistry and Biochemistry, The Ohio State University, Columbus, OH, USA

Received July 22, 2013; Revised and Accepted November 21, 2013

The actin-binding and bundling protein, plastin 3 (PLS3), was identified as a protective modifier of spinal muscular atrophy (SMA) in some patient populations and as a disease modifier in animal models of SMA. How it functions in this process, however, is not known. Because PLS3 is an actin-binding/bundling protein, we hypothesized it would likely act via modification of the actin cytoskeleton in axons and neuromuscular junctions to protect motoneurons in SMA. To test this, we examined the ability of other known actin cytoskeleton organizing proteins to modify motor axon outgrowth phenotypes in an *smn* morphant zebrafish model of SMA. While PLS3 can fully compensate for low levels of *smn*, cofilin 1, profilin 2 and α-actinin 1 did not affect *smn* morphant motor axon outgrowth. To determine how PLS3 functions in SMA, we generated deletion constructs of conserved PLS3 structural domains. The EF hands were essential for PLS3 rescue of *smn* morphant phenotypes, and mutation of the Ca^{2+}-binding residues within the EF hands resulted in a complete loss of PLS3 rescue. These results indicate that Ca^{2+} regulation is essential for the function of PLS3 in motor axons. Remarkably, PLS3 mutants lacking both actin-binding domains were still able to rescue motor axons in *smn* morphants, although not as well as full-length PLS3. Therefore, PLS3 function in this process may have an actin-independent component.

INTRODUCTION

Spinal muscular atrophy (SMA) is an autosomal recessive disorder resulting from low levels of the survival motor neuron (SMN) protein due to loss or mutation of the survival of motor neuron 1 (SMN1) gene (1). While one of ~40–60 people are carriers of mutations or deletions of SMN1, SMA affects 1 in 6000–10 000 live births and is, therefore, the leading genetic cause of infant mortality (2–8). SMA results in a progressive, selective degeneration of α-motoneurons in the anterior horn of the spinal cord leading to atrophy of proximal muscles. The severity of the disease is primarily determined by levels of SMN protein produced from the almost identical SMN2 gene (1,5–7,9). Owing to disruption of an exonic splice enhancer (1,10–14), only 10–15% of SMN transcripts produced from SMN2 are full length (10), whereas the rest of transcripts lack exon 7 and, therefore, are unstable.

SMN2 copy number generally correlates with disease classification, as type zero patients typically have a single copy of SMN2, type I have two copies, type II and III have three to four copies and type IV have four to eight copies (5,15,16). However, there are additional factors of heterogeneity within the SMA population, as some patients with only two copies of SMN2 have presented with a disproportionately mild type IIIB phenotype of SMA (17). Discordant families have also been described in which siblings have the same genetics, but present with different phenotypes, with some siblings affected and others unaffected (18–24). This suggests that modifiers other than SMN may exist.

Plastin 3 (PLS3), an actin-binding and bundling protein, was identified as a protective modifier of SMA in a transcriptome-wide differential expression screen from lymphoblastoid cell RNA obtained from discordant SMA family members (22). Enhanced expression of PLS3 in the blood was detected in female siblings that were protected from disease symptoms (22). Another group has confirmed this finding in post-pubertal females (23), while others have shown that PLS3 expression is not found in lymphoblasts from all protected siblings in discordant SMA families (24). Thus, additional phenotypic modifiers of the disease are likely.

*To whom correspondence should be addressed. Tel: 614-292-5113; Fax: 614-292-5379; Email: christine.beattie@osumc.edu

In both transient and genetic zebrafish models of SMA, motor axons are branched and truncated (25,26). PLS3 expression is able to rescue motor axon defects in both cultured neurons and in zebrafish embryos (22). In a genetic model of SMA in zebrafish, PLS3 was able to compensate for low levels of Smn in both synapse morphology and motor function (27). Furthermore, PLS3 expression has been shown to be protective in other SMA animal models (27–29). In mice, PLS3 expression increased the number of vesicles available in the readily releasable pool at the synapse, improved motor behavior and modestly rescued survival (29). While these data support PLS3 as a true modifier of SMA, the mechanism by which PLS3 achieves these outcomes remains unknown.

Plastins are evolutionarily conserved, versatile modulators of the actin cytoskeleton, which play an important role in cell migration, adhesion and endocytosis. The three family members, PLS1 (I-plastin), LCP1 (L-plastin or PLS2) and PLS3 (T-plastin), all have similar modular structural domains, but are differentially expressed. For clarity, these family members will be referred to as PLS1, PLS2 and PLS3. PLS1 is expressed in absorptive intestinal and kidney cells (30), PLS2 is predominantly found in hematopoetic and cancer cells (31–33), and PLS3 is expressed in solid tissues (33,34). All members of the plastin family have two N-terminal EF hand motifs and two C-terminal actin-binding domains (ABDs), each composed of two calponin homology (CH) domains. Bundling of actin requires binding of each ABD to an individual actin filament (35), and therefore, plastin lacking the C-terminal ABD (ABD2) cannot bundle actin (36). To examine the function of plastin that is responsible for the modifier phenotype in SMA, we investigated the ability of the full-length PLS3 and its individual domains to rescue motor axon defects in zebrafish *smn* morphant embryos. Additionally, we examined whether other important actin-modifying proteins were able to affect axon outgrowth phenotypes. Surprisingly, our results support a mechanism for PLS3 in SMA beyond that of actin binding.

RESULTS

Plastin 3 fully rescues *smn* morphant motor axon defects

We had previously demonstrated that decreasing Smn levels in zebrafish transiently resulted in motor axon outgrowth defects (25). Characterization of these defects revealed that motor axons were truncated and/or branched (37). This was confirmed in a genetic model of SMA in zebrafish thus validating these defects as a read-out of low Smn levels (26). PLS3 has been reported to rescue motor axon defects resulting from low SMN levels both *in vitro* and *in vivo* (22). We first sought to determine whether a given dose of PLS3 could rescue *smn* morphant motor axons at levels that were not statistically different than control morpholino levels. Previous results were obtained at 125 pg/nL (22), but in the present study all experiments were conducted at higher doses of 250 pg/nL, except where otherwise noted. Human PLS3 was cloned into pcDNA-DEST40, a vector with C-terminal V5 and 6xHis tags. PLS3 mRNA with V5 and 6xHis tags generated from this vector, as well as untagged PLS3 mRNA, was co-injected with *smn* MO. No differences between tagged and untagged PLS3 were observed (data not shown); 250 pg/nL was chosen because it was found to fully rescue axon defects so that the embryos were indistinguishable from controls (Fig. 1A and B).

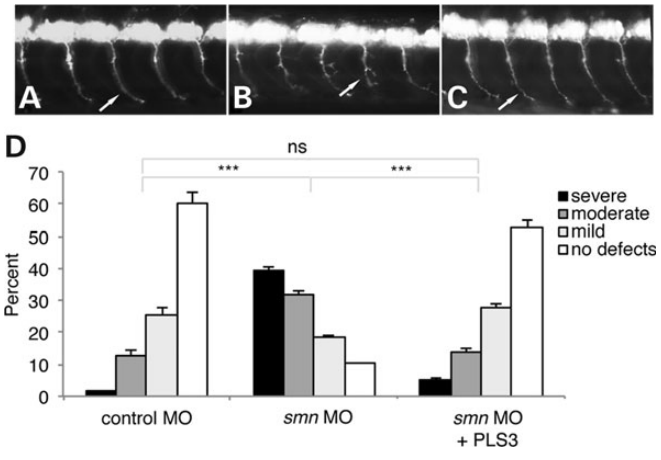

Figure 1. *Expression of PLS3 rescues motor axon defects in smn morphants.* Representative images of ventral axons in 28 hpf Tg(*mnx1:0.6hsp70:EGFP*) embryos injected with (**A**) control MO, (**B**) *smn* MO and (**C**) *smn* MO with 250 pg PLS3 mRNA. (**D**) Quantitation and statistical analysis of the motor axon defects using a Mann–Whitney non-parametric rank test. The arrows in (A)–(C) indicate individual motor axons. ns, non-significant; $^{***}P \leq 0.001$.

Cofilin, profilin and α-actinin cannot rescue *smn* morphant axon defects

To determine whether PLS3 was unique among actin-modifying proteins in its ability to affect *smn* morphant axon defects, we examined whether other proteins known to bind and modify actin filaments would have any effect on *smn* morphant axon defects. We reasoned if PLS3's ability to bind and bundle actin filaments was responsible for rescuing truncated and branched motor axons, other actin modifying proteins might influence motor axon degeneration in SMA as well. Because many dozens of actin-binding proteins are present *in vivo*, testing all or even a substantial fraction of them was impossible within one study. Therefore, we chose to examine profilin, cofilin and α-actinin, three essential actin modifiers both structurally similar and dissimilar to plastin, and outside of the plastin family of proteins (Fig. 2A). Cofilin and profilin are essential proteins that regulate actin filament turnover by promoting disassembly of old ADP-rich filaments, and recharge of actin monomers with ATP and new filament assembly, respectively (37–39). Similar to plastins, α-actinin1 (ACTN1) is an actin-bundling protein that contains tandem CH domains that form an actin-binding domain and a pair of EF hand motifs regulated by Ca^{2+} (Fig. 2A). Antiparallel dimers of α-actinin form rod-shaped structures by interaction between adjacent spectrin domains, while the flexible N-terminal actin-binding domains bind and cross-link adjacent actin filaments (40).

We first asked whether profilin 2, which promotes actin filament polymerization by adding monomeric G-actin onto the end of the growing actin filaments, could substitute for PLS3. We found that profilin 2 was unable to rescue motor axon defects of *smn* morphants to any degree (Fig. 2B and C). Similarly, we found that cofilin 1, an actin filament severing and depolymerizing protein, did not alter *smn* morphant axons (Fig. 2B and C). Finally, we tested whether ACTN1 could rescue axon defects. In spite of

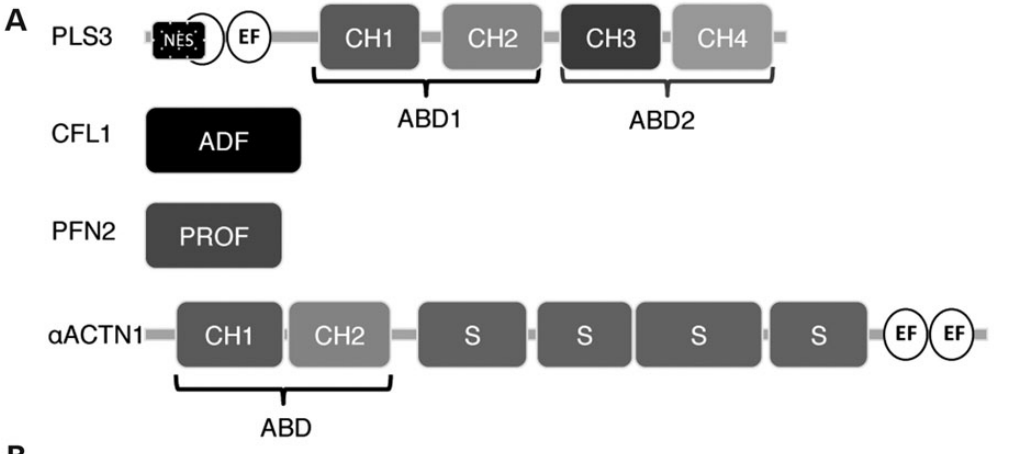

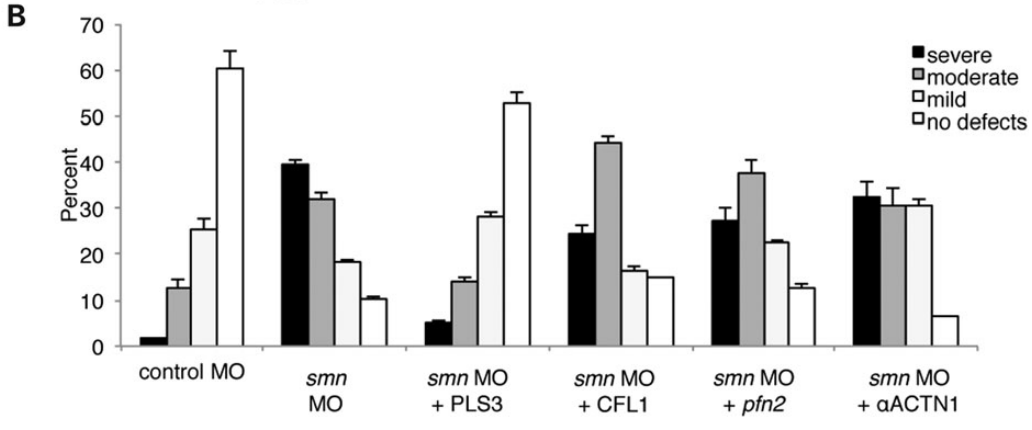

C

p-value	compared to control MO	compared to *smn* MO	compared to *smn* MO + PLS3
smn MO + CFL1	***	ns	***
smn MO + pfn2	***	ns	***
smn MO + αACTN1	***	ns	***

Figure 2. Actin-binding proteins are unable to rescue motor axon defects in smn morphants. (**A**) Structural motifs in actin-binding protein constructs. PLS3 contains N-terminal EF hand motifs, and two C-terminal actin-binding domains, each composed of two calponin homology domains. αACTN1 is structurally similar to PLS3, with an N-terminal ABD, composed of two calponin homology domains, and two C-terminal EF hand motifs. αACTN1 also has central spectrin (S) repeat domains. CFL1 is composed of one actin depolymerization factor domain, and PFN2 is composed of a profilin domain. All constructs had V5 and 6xHis C-terminal tags. Constructs are drawn to scale. (**B**) Co-injection of *smn* MO with RNA encoding actin-binding proteins. (**C**) Table depicting statistical significance determined by Mann–Whitney analysis of distribution between injection conditions. Significance is set at $^{*}P \leq 0.05$, $^{**}P \leq 0.01$, $^{***}P \leq 0.001$ and ns indicates not significant.

substantial structural and functional similarity to PLS3, ACTN1 did not rescue *smn* morphant motor axons (Fig. 2B and C). Therefore, none of the actin modifying proteins tested was able to compensate for PLS3 function in *smn* morphant motor axons.

PLS2, but not PLS1, can substitute for PLS3

Three members of the plastin family of proteins have been identified: PLS3 T-plastin, PLS2 (L-plastin, LCP1) and PLS1 (I-plastin). These proteins have ∼73% amino acid identity, share all conserved structural motifs and the ability to cross-link actin filaments into tight bundles. Yet, they are differentially expressed and demonstrate some functional differences (41–43). To determine whether PLS2 or PLS1 could substitute for PLS3 to rescue motor axon defects in *smn* morphant embryos, we co-injected PLS2 or PLS1 mRNA with *smn* MO (Fig. 3A). Intriguingly, PLS2 was able to substitute for PLS3, whereas PLS1 provided no significant improvement of motor axon defects. Because 250 pg of PLS1 was not sufficient to rescue motor axons, we tested an increased dose of 500 pg for both PLS2 and PLS1 (Fig. 3A and B). PLS1 still showed no significant ability to rescue motor axon outgrowth in *smn* morphants at an increased dosage, but PLS2 was now able to fully rescue normal axon morphology. Thus, PLS2 can rescue motor axons in *smn* morphants, albeit less efficiently than PLS3, while PLS1 showed no ability to rescue these defects.

Acting binding is not sufficient to rescue motor axon defects

To examine which of the conserved plastin motifs is critical for PLS3's function in rescuing motor axon outgrowth in *smn* morphants, we generated several PLS3 deletion constructs (Fig 4).

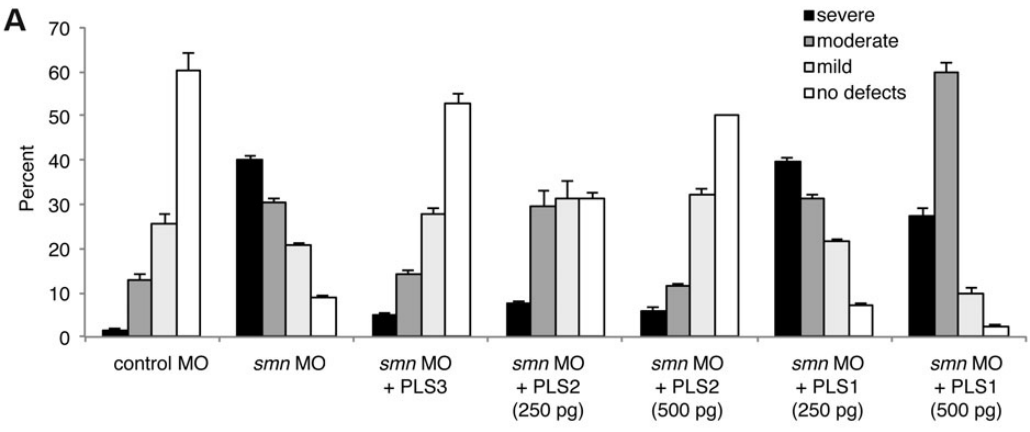

B

p-value	compared to control MO	compared to *smn* MO	compared to *smn* MO + PLS3
smn MO + PLS3	ns	***	
smn MO + PLS2	ns	***	ns
smn MO + PLS1	***	ns	***

Figure 3. PLS2, but not PLS1, rescues motor axon defects in smn morphants. (**A**) Co-injection of *smn* MO with plastin family members. PLS2 and PLS1 rescue was tested at 250 and 500 pg (**B**) Table showing statistical significance between injection conditions as determined by Mann–Whitney analysis. PLS2 and PLS1 statistics are both shown at 500 pg doses.

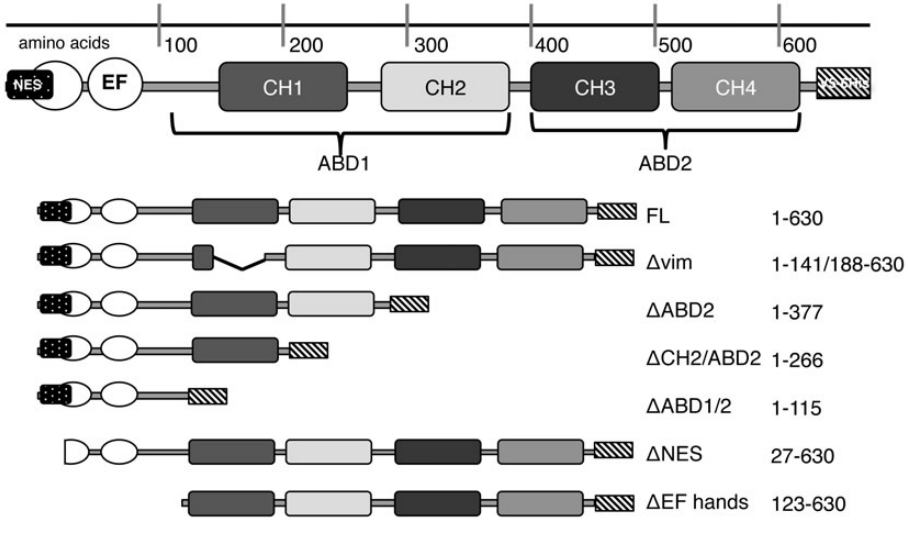

Figure 4. Schematic diagram of human PLS3 deletion constructs. PLS3 is a 630 amino acid protein with several evolutionarily conserved structural motifs. The full-length (FL) construct contains a nuclear export signal that overlaps with an N-terminal EF hand motif. The C-terminus contains a pair of actin-binding domains, ABD1 and ABD2, each composed of two calponin homology (CH) domains. All constructs have V5 and 6xHis tags at the C-terminus.

PLS2 has been described to interact with the intermediate filament protein vimentin via a part of its ABD1 domain (44). To determine whether PLS3 function in *smn* morphant motor axons was also due to such an interaction, we generated a PLS3 construct lacking the putative vimentin interaction motif (Δvim). This construct was able to fully rescue axon defects similar to full-length PLS3 (Fig. 5A and C), suggesting that interaction of PLS3 with vimentin does not contribute to the mechanism by which PLS3 rescues *smn* morphant axons.

Because plastin has a well-described role in actin filament bundling, we next tested whether deletion of the actin-binding domains would affect PLS3-mediated rescue of *smn* morphant axons. PLS3 acts to cross-link actin filaments by binding separate filaments with each of its actin-binding domains, ABD1 and ABD2 (35). Thus, loss of ABD2 results in an inability to cross-link actin filaments (36). Therefore, we tested whether actin-bundling function of PLS3 was required for *smn* morphant motor axon outgrowth by co-injecting *smn* MO with ΔABD2 mRNA. Surprisingly, we observed a significant ability of ΔABD2 to rescue *smn* morphant motor axons (Fig. 5A and C). An increase in the number of fish exhibiting mild defects in comparison with *smn* MO alone reflects an improved axon morphology. While this

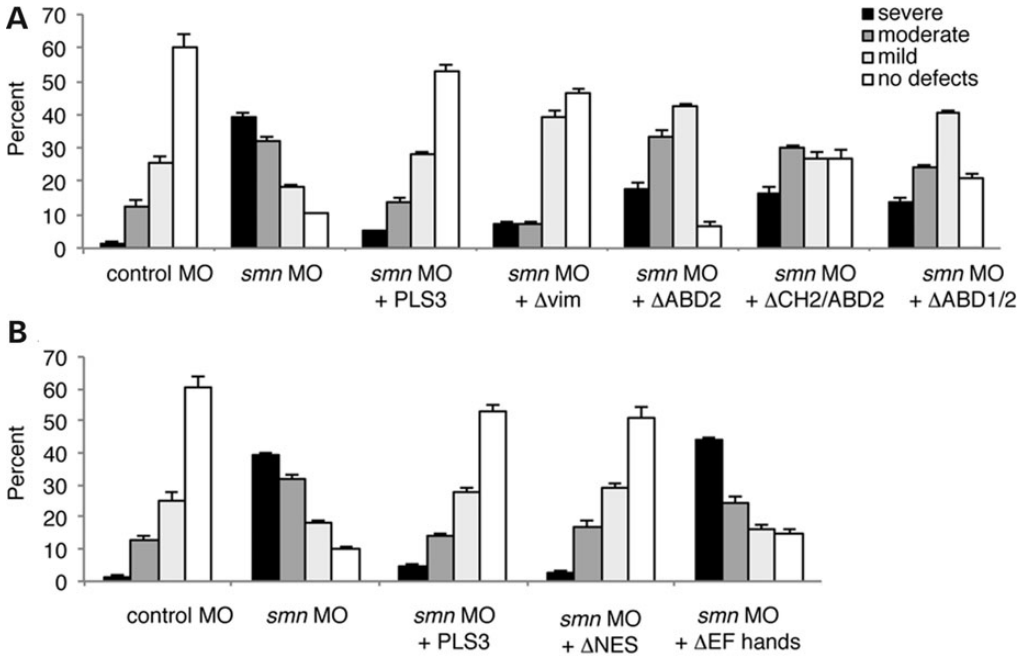

C

p-value	compared to control MO	compared to *smn* MO	compared to *smn* MO + PLS3
smn MO + Δvim	ns	***	ns
smn MO + ΔABD2	***	**	***
smn MO + ΔCH2/ABD2	***	**	**
smn MO + ΔABD1/2	***	***	***
smn MO + ΔNES	ns	***	ns
smn MO + ΔEF hands	***	ns	***

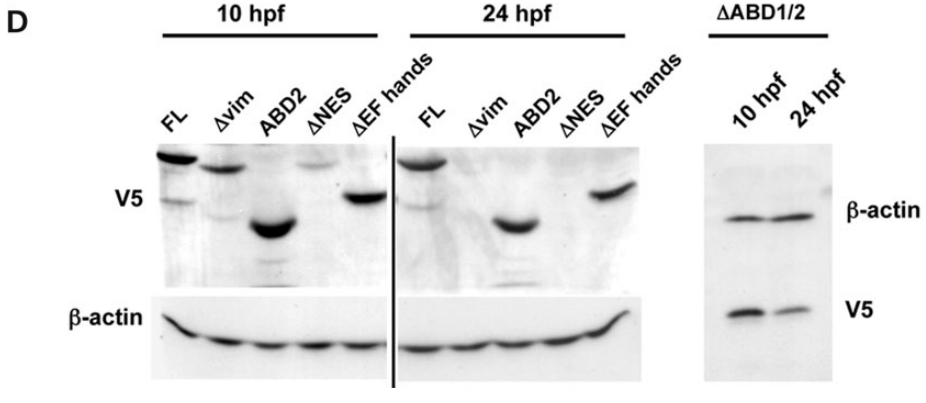

Figure 5. EF hands are required for PLS3 function in smn morphant motor axons. (**A**) Motor axon defects observed in *smn* morphants with 250 pg injection of PLS3 C-terminal deletions: Δvim, ΔABD2, ΔCH2/ABD2 and ΔABD1/2 mRNA (**B**) Motor axon defects observed in *smn* morphants with 250 pg injection of PLS3 N-terminal deletions: ΔNES and ΔEF hands mRNA (**C**) Table showing statistical significance between injection conditions as determined by Mann–Whitney analysis. (**D**) Western blots from 10 and 24 hpf embryos injected with RNA from PLS3 constructs at the one-cell stage as detected by V5 expression. β-Actin is used as a loading control. Owing to its small size, ABD1/2 was run separately on a 15% polyacrylamide gel, whereas all other constructs were run on a 7.5% gel.

construct was not able to rescue the phenotype as well as full-length PLS3, we concluded that the bundling function of PLS3 is not solely responsible for rescuing *smn* morphant axons.

To determine whether PLS3 interaction with filamentous actin was necessary for rescue, we deleted half of ABD1 in addition to ABD2 (ΔCH2/ABD2) as well as the entirety of both actin-binding domains (ΔABD1/2), thus completely ablating not only bundling, but also binding of the constructs to actin. Surprisingly, both constructs were capable of rescuing axon morphology (Fig. 5A and C). Similar results were obtained with ΔABD2 and ΔCH2/ABD2 constructs, which lacked C-terminal tags (data not shown). Additionally, an increased dosage of

ΔABD1/2 was not sufficient to fully reproduce the effects of full-length PLS3 (Supplementary Material, Fig. S1). Thus, we observed significantly improved axon morphology with ΔABD1/2, albeit the defects were greater than those observed in the full-length PLS3 injected morphants. This observation suggests that PLS3's function in *smn* morphant embryos might involve an additional mechanism unrelated to its interaction with actin.

EF hands are necessary for PLS3 function in *smn* morphants

To address what other PLS3 domains were important for motor axon development, we next examined the N-terminus of PLS3. Several important structural and regulatory motifs are found in the N-terminus of plastin isoforms. Phosphorylation of serines five and seven regulates PLS2 localization to active sites of actin filament assembly (45,46). Although a conserved serine residue is found at position seven of PLS3, no known role for phosophorylation of this site in PLS3 has been described. Additionally, a nuclear export signal (NES) overlaps the first EF hand motif in PLS3, promoting its cytoplasmic localization (47). The signal is weaker in PLS2, which shuttles between the nucleus and cytoplasm. Furthermore, the N-terminus also contains two EF hands, which are calcium-binding regulatory motifs (48). To determine whether any of these N-terminal motifs were necessary for PLS3 function in motor axon outgrowth in *smn* morphants, we generated two deletion constructs, ΔEF hands and ΔNES. ΔEF hands are a deletion of both EF hands and all amino acids to the N-terminus of these motifs (Fig. 4). ΔNES is a smaller deletion of only the NES and all the amino acids N-terminal to this motif (Fig. 4). Interestingly, co-injection of *smn* MO with ΔEF hands mRNA failed to show any significant differences from *smn* MO alone (Fig. 4B and C). Increased dose of ΔEF hands mRNA (Supplementary Material, Fig. S1) as well as the ΔEF hands construct lacking the C-terminal V5 and 6xHis tags (data not shown) did not demonstrate any significant ability to rescue axons. Therefore, we concluded that some part of the N-terminus was necessary for the function of PLS3 to rescue morphological axon defects in *smn* morphants. In striking contrast with ΔEF hands, ΔNES mRNA was able to completely rescue axon defects in *smn* morphant embryos (Fig. 5B and C). Therefore, the ability of PLS3 to rescue motor axon defects requires amino acids 27–82, encompassing half of the first EF hand and the entire second EF hand motif. Because ΔNES could completely rescue axon defects but ΔEF hands could not, we eliminated potential roles for serine 7 phosphorylation as well as the NES. Although the EF hand motifs are essential and alone result in partial rescue of the *smn* MO phenotype, the full-length PLS3 construct is able to produce a complete rescue. Thus, the EF hand motifs in the N-terminus of PLS3 are necessary, but not sufficient for PLS3 to function in motor axon morphology in *smn* morphant embryos.

To ensure that all of the RNA constructs could indeed generate protein *in vivo*, we performed western blots from embryos injected with RNA at the 1-cell stage (Fig. 5D). At 10 hpf, all forms were expressed although ΔNES at a lower level. At 24 hpf, protein was observed for all forms except ΔNES and Δvim. However, both of these RNAs rescued motor axons suggesting that the amount of protein generated was sufficient to rescue. The RNA that failed to rescue, ΔEF hands, was expressed at both time points.

Subcellular localization of PLS3 deletion mutants

PLS3 has functional roles in both the cytoplasm and the nucleus (49,50). Cellular localization of PLS3 is at least in part, controlled via its NES, which is removed in both the ΔNES and ΔEF hands constructs. This removal might result in their excessive accumulation in the nucleus and consequent depletion from the cytoplasm. Although the ΔNES construct is able to rescue motor axon outgrowth, the function of PLS3 necessary for motor axons could be a nuclear role. To test this, we transfected human embryonic kidney (HEK293) cells with V5-tagged forms of all constructs and performed immunofluorescent labeling against the V5 tags and filamentous actin (Fig 6). Upon transfection with PLS3, we did observe cellular rounding and some loss of cellular adherence, as has previously been reported (41). However, PLS3 was primarily located in the cytoplasm and co-localized with filamentous actin at the peripheral edges of the cells (Fig. 6C and D). Although all constructs were found in the cytoplasm, an increase in the amount of nuclear PLS3 was observed in ΔNES and ΔEF hands constructs lacking the NES (Fig. 6G–J). From this, we could rule out nuclear PLS3 functions as a requirement for rescue of motor axon outgrowth in *smn* morphants.

Ca^{2+} binding is critical for PLS3 function in *smn* morphants

Because EF hands are known to bind calcium to regulate protein function, we next examined whether PLS3 calcium binding was necessary for its ability to rescue motor axon outgrowth defects. We mutated each residue of both EF hands that contacts a calcium ion, as has previously been reported with α-actinin (51) (Fig. 7A). For the first Ca^{2+}-binding site, we mutated D25A, N27A, N29A, F31A, C33A, E36A in the context of the full-length PLS3 cDNA to create the construct EF mut 1. The second binding domain was mutated to D65A, N67A, D69A, K71A, S73A, E76A to create the construct EF mut 2. Finally, we generated a construct with all of the previously described mutations, termed EF mut 1 + 2. Interestingly, none of these mutated Ca^{2+}-binding EF hand constructs was able to significantly rescue *smn* morphant motor axon outgrowth defects (Fig. 7B and C). To verify these experiments, we injected the DNA constructs directly into one-cell stage zebrafish (as opposed to injecting RNA) and found that full-length PLS3, but not PLS3 with mutated Ca^{2+}-binding EF hands, could rescue the motor axons (data not shown). Thus, calcium binding appears to be essential for PLS3 function in motoneuron axon outgrowth.

PLS3 function in actin binding and bundling

To define whether actin-binding and bundling functions of PLS3 are affected by Ca^{2+}, we examined the ability of full-length PLS3 and PLS3 mutants to bind and bundle actin *in vitro* using light scattering and a co-sedimentation assay across a range of free Ca^{2+} concentrations (pCa 8.5–3.8). PLS3 binding was assessed by its appearance in the pellet fractions together with filamentous actin after a high-speed centrifugation (200 000*g*). As expected, binding of ΔEF hands and EF mut 1 + 2 constructs to actin was not affected by Ca^{2+} (Fig. 8A and B). However, binding of full-length PLS3 to actin was also unaffected across

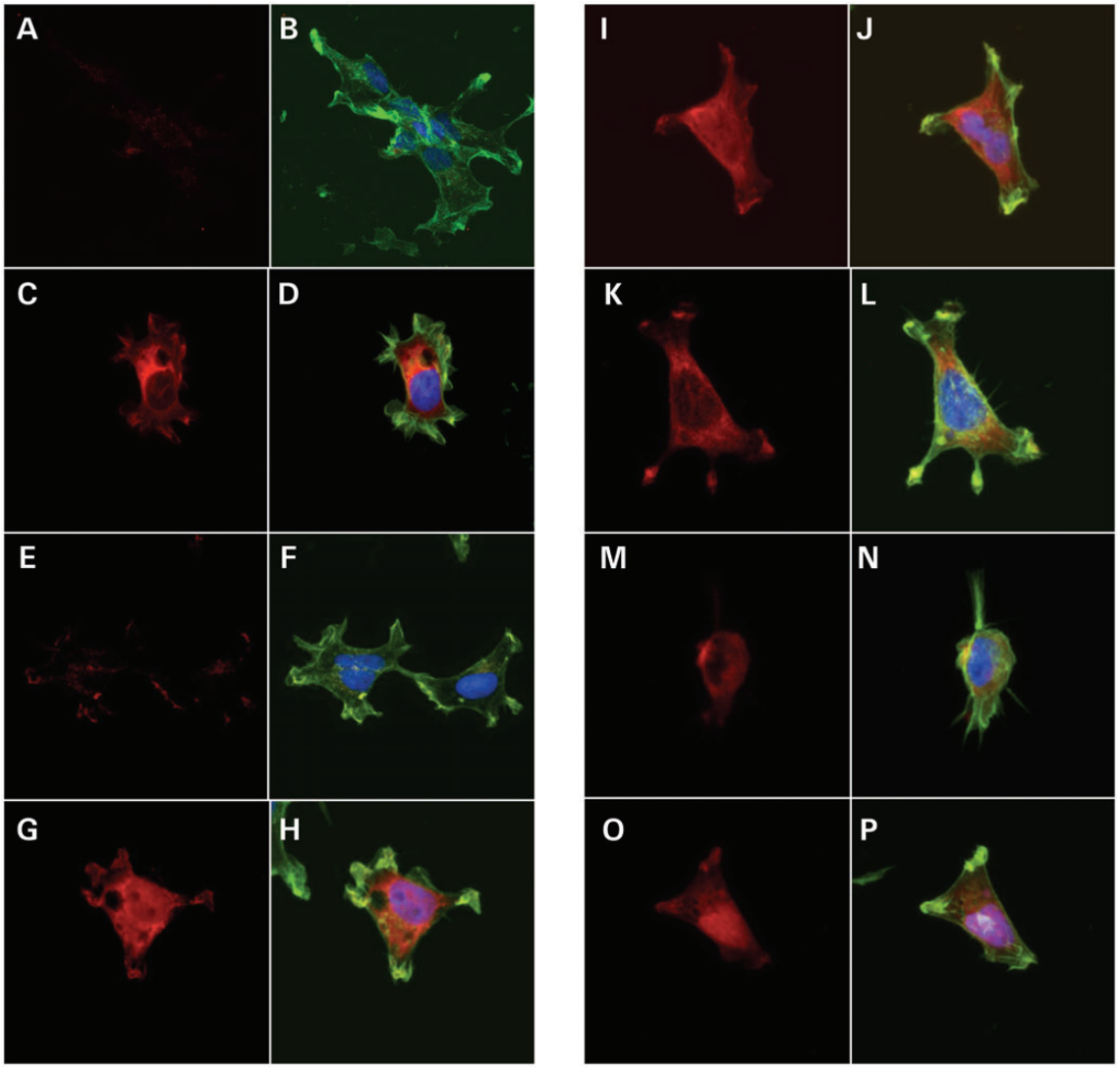

Figure 6. Immunofluorescence of PLS3 colocalization with filamentous actin in HEK293 cells. PLS3 constructs are stained with antibody to C-terminal V5 tag (red). Filamentous actin is labeled with AlexaFluor488-phalloidin conjugate (green). DAPI (blue) labels the nucleus, (**A** and **B**) empty pDEST40 vector, (**C** and **D**) FL PLS3, (**E** and **F**) FL PLS3 pDEST40 (labeled only with secondary antibody, control for staining specificity), (**G** and **H**) ΔNES, (**I** and **J**) ΔEF hands, (**K** and **L**) Δvimentin interact, (**M** and **N**) ΔABD2, and (**O** and **P**) ΔABD1/2. All imaging was performed with the same laser intensity.

the entire range of Ca^{2+} concentrations examined, suggesting that interaction of at least one of the PLS3 ABDs with actin (ABD1 or ABD2) is not affected by Ca^{2+} (Fig. 8A and B). Full-length PLS3 has notably lower affinity to actin than both EF hand mutants, presumably due to a partial inhibitory effect of EF hands at any concentration of Ca^{2+} tested.

Bundling of actin filaments can be efficiently monitored by an increase in light scattering upon formation of large filament assemblies. Addition of PLS3 to pre-formed actin filaments caused an immediate increase in light scattering that took approximately an hour to fully develop (Fig. 8C). A subsequent addition of a high Ca^{2+} concentration (pCa 4.0) caused a prompt drop of light scattering back to the initial level indicating that PLS3 bundling activity was abolished (Fig. 8C). These results were further confirmed using low-speed centrifugation (17 000*g*) of actin bundles formed in the presence of PLS3 constructs. In this assay, single filaments of actin remained in the supernatant, while actin bundles were found in the pellet fraction. Bundling of actin by full-length PLS3 was dependent upon Ca^{2+} concentration, whereas bundling by ΔEF hands and EF mut 1 + 2 proteins were insensitive to Ca^{2+} (Fig. 8D and E). At low Ca^{2+} concentration (pCa 8.5–5.3), PLS3 was able to bundle actin filaments, but at higher Ca^{2+} concentration (pCa < 5.0), PLS3 failed to bundle actin. Therefore, the inability of both constructs with altered/deleted EF hands to rescue the *smn* MO axon phenotype may directly relate to their inability to be regulated by Ca^{2+}.

Since ΔABD1/2 was able to partially rescue motor axons of *smn* morphants (Fig. 5A and C), we examined whether this construct retains a residual activity toward actin. Without actin-binding domains, we predicted that this construct would be unable to interact with actin. Indeed, we found that ΔABD1/2 was unable to bind or bundle actin under any conditions (Fig. 8A and D).

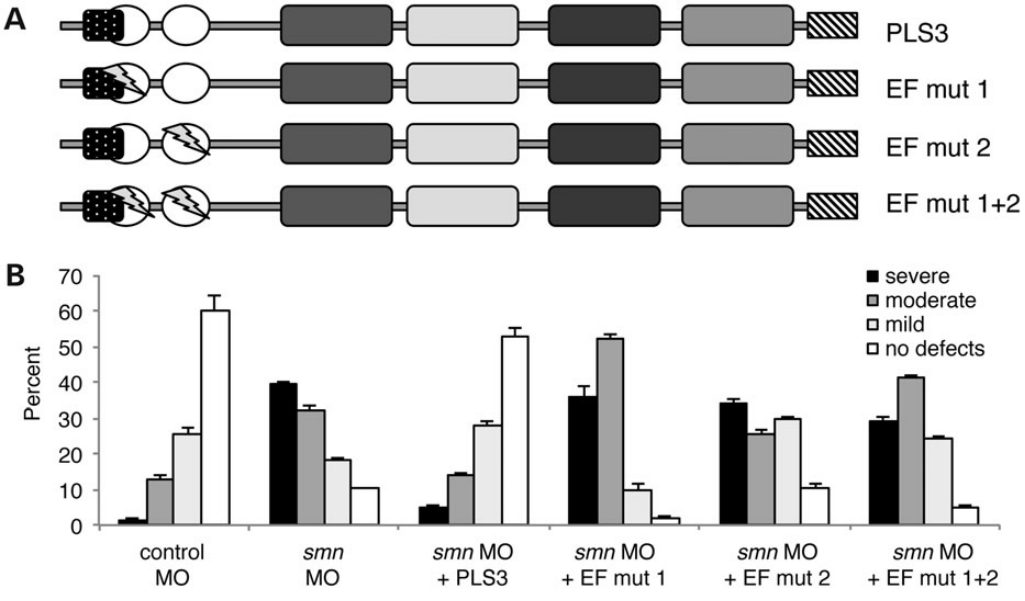

C

p-value	compared to control MO	compared to *smn* MO	compared to *smn* MO + PLS3
smn MO + EF mut 1	***	ns	***
smn MO + EF mut 2	***	ns	***
smn MO + EF mut 1+2	***	ns	***

Figure 7. Ca^{2+} binding to EF hands is required for PLS3 function in smn-depleted motor axons. (**A**) Schematic depicting PLS3 constructs containing point mutations for Ca^{2+} binding residues in the EF hands of PLS3. EF mut 1 contains the following point mutations: D25A, N27A, N29A, F31A, C33A, E36A. EF mut 2 contains D65A, N67A, D69A, K71A, S73A, E76A. EF mut 1 + 2 contains all of the mutations mentioned. (**B**) Motor axon defects observed in *smn* morphants with 250 pg mRNA injection of EF hand point mutants: EF mut 1, EF mut 2 and EF mut 1 + 2. (**C**) Statistical table depicting significance between injection groups as determined by Mann–Whitney analysis.

Thus, we have demonstrated that PLS3 actin bundling is inhibited by a free Ca^{2+} concentration >10 μM (pCa < 5.0). Our data support a mechanism by which Ca^{2+} binding directly to PLS3 via its EF hand motifs regulates actin bundling (Fig 9).

DISCUSSION

Motor axon outgrowth is a key component of nervous system development. We have shown in both transient and genetic models of SMA that motor axon outgrowth is affected (25,26), and that this is a reflection of aberrant motoneuron development (26). To gain insight into how SMN is affecting motoneuron development, we have examined the protein PLS3, which has been shown in animal models of SMA and in some human studies to be a modifier of SMA phenotypes, especially those involved in motor function (22,26,29). Previously, we had shown that PLS3 expression could rescue the motor axon defects caused by transient knockdown of Smn (22) and driving PLS3 in motoneurons in a genetic model of SMA could rescue neuromuscular junctions and movement defects (27). The goal of this current study was to dissect the functional requirements that are needed for PLS3 to rescue the motor axon defects using the *smn* morphant model.

PLS3's best-described function has been as an actin-bundling protein (52), but other functions have also been ascribed to PLS3 and other plastin family members (41,42,49,50,53 –57). However, very little is known about PLS3 function in the developing nervous system. From our structure-function data using PLS3 deletion constructs, we definitively showed that PLS3 EF hand motifs are required for PLS3 function in developing motoneurons. By mutating all residues that interact with Ca^{2+} ions within the EF hands, we determined that Ca^{2+} binding to the EF hand motifs is essential for PLS3 function in motoneuron development. Thus, these data define a novel role for Ca^{2+} regulation in PLS3 function in motor neuron development. Calcium dysregulation has previously been implicated in SMA. Analysis of different muscles in SMA mice has revealed that in some muscles (e.g. TVA, TA) neurotransmission is decreased and the kinetics of the postsynaptic response is slowed (58,59). Interestingly, there is also altered calcium homeostasis at affected NMJs in these mice (59). Analysis of cultured motor axonal growth cones from SMA mice also revealed reduced local calcium influx and reduced voltage-gated calcium channels [Cav2.2, (60)]. These studies suggest that calcium dysregulation in the growth cone during motor axon outgrowth is altered in SMA. Glial cells may also have calcium defects, as iPS cells from SMA mice induced to become glial cells displayed altered basal calcium levels (61). Calcium transients occur locally at the tips of extending axon branches and growth cones in cultured neurons and are critical for filopodial dynamics and axonal growth (62). We have previously shown that filopodial dynamics are affected *in vivo* in *smn* mutant zebrafish (26). One possibility is that calcium

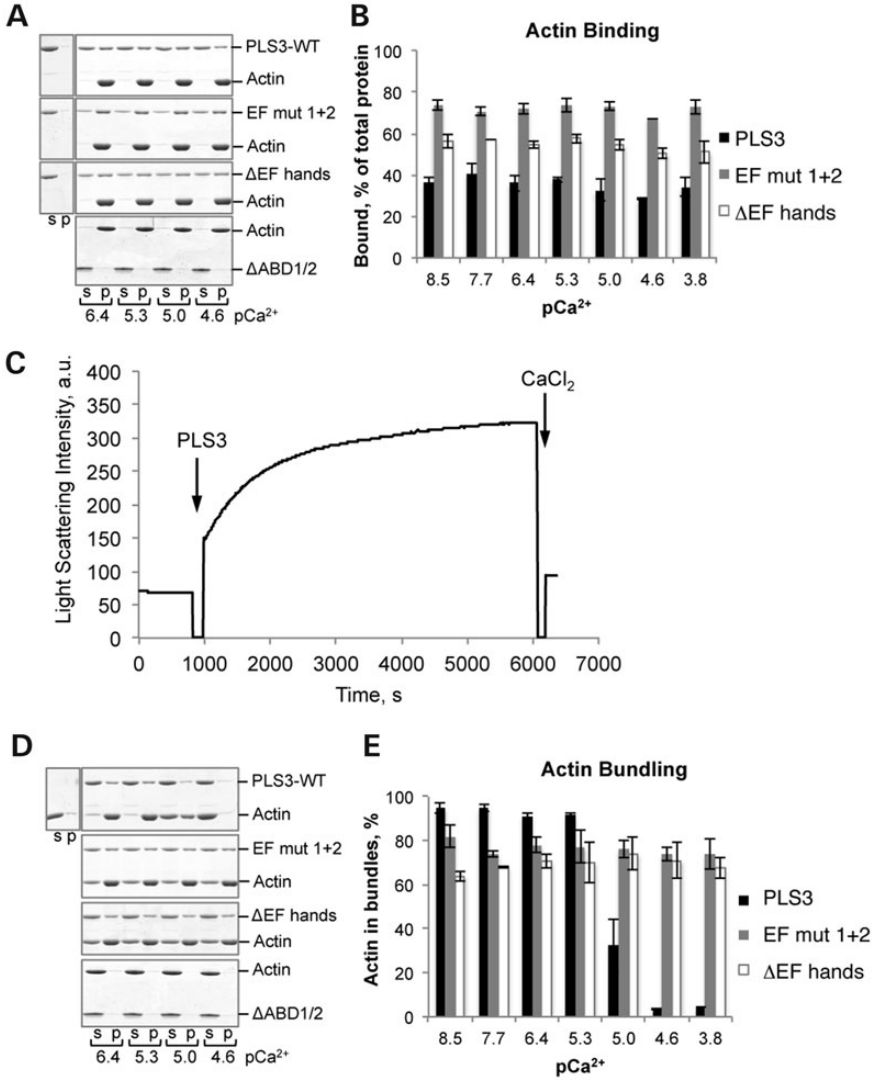

Figure 8. Ca^{2+} inhibits actin-bundling activity of PLS3, but has no effect on actin binding. (**A**) Binding of 2 μM of PLS3, EF mut 1 + 2, ΔEF hands and 30 μM of ΔABD1/2 to 5 μM of F-actin in the presence of different concentrations of free Ca^{2+} was assessed by the high speed co-sedimentation assay (200 000*g* for 30 min) followed by SDS–PAGE analysis of pellet and supernatant fractions. Pellets (p) contain F-actin and bound PLS proteins; supernatants (s) contain unbound PLS. Sedimentation of PLS3 and its mutants in the absence of actin is shown as a control on the left. The positions of wild-type PLS3, EF mut 1 + 2, and ΔEF hands and actin are marked on the right. The experiment was conducted under different pCa^{2+} 8.5, 7.7, 6.4, 5.3, 5.0, 4.6 and 3.8; but only pCa^{2+} 6.4–4.6 range is presented in (A). (**B**) The amounts of PLS3 proteins bound to actin from three independent experiments were expressed as the per cent of the corresponding total PLS3 protein (combined PLS3 in the supernatant and pellet) and shown on the graph. Error bars, SEM. (**C**) Time course of change in light scattering intensity of 5 μM F-actin solution was recorded by spectrofluorometer with emission and excitation wavelengths set at 330 nm. Addition of PLS3 (2 μM) to F-actin increased light scattering of the sample reflecting bundling of actin filaments by PLS3. Subsequent addition of $CaCl_2$ (0.1 mM free Ca^{2+}, pCa^{2+} 4.0) reduced the signal to a nearly initial level. (**D**) Bundling of F-actin (5 μM) by PLS3, EF mut 1 + 2, ΔEF hands, and ΔABD (2, 2, 2, and 30 μM, respectively) in buffers with various concentrations of Ca^{2+} was assessed by low-speed sedimentation (17 000*g* for 15 min) followed by the SDS–PAGE analysis. Under these sedimentation conditions, F-actin bundles were found in the pellet fraction (p), whereas unbundled actin filaments remained in the supernatant (s). Sedimentation of F-actin alone is shown on the left as a control for unbundled actin. (**E**) Amount of bundled F-actin in pellet was expressed as a per cent of total actin (combined supernatant and pellet) and shown on the graph. Error bars, SEM ($n = 3$).

dysregulation in the growth cone or in the environment around the growth cone could affect axon outgrowth through a calcium-dependent PLS3 function.

Because Ca^{2+} is known to regulate PLS2's binding and bundling activity toward filamentous actin (63) and Ca^{2+} regulation of PLS3 had not been definitively determined (36,43), we examined whether the actin-binding domains of PLS3 were necessary for PLS3 activity in axons. Our results show that PLS3 lacking actin-binding domains, ΔABD1/2, still retains some function within motor axons. We confirmed that this construct does indeed lack any ability to bind actin via a co-sedimentation assay. This retained function within motor axons, in spite of a lack of actin binding, suggests that PLS3 function in *smn* morphant axons may be independent of its actin activity. This result was rather surprising since the best-characterized activity of PLS3 is binding and bundling actin (52) and actin filament dynamics are crucial for axon outgrowth (64). Interestingly, none of the other actin-modifying proteins (Pfn2, CFL1 and α-ACTN1) that we

construct		rescues *smn* MO axon defects	binds actin	bundles actin	ability to bind Ca^{2+}	actin bundling negatively regulated by Ca^{2+}
PLS3		+++	+++	+++	+++	+++
ΔABD1/2		++	-	-	+++	-
ΔEF hands		-	+++	+++	-	-
EF mut 1+2		-	+++	+++	-	-

Figure 9. *Summary of PLS3 functional activity.* Full-length PLS3, ΔABD1/2, ΔEF hands, and EF mut 1 + 2 are described in terms of their ability to rescue of *smn* morphant motor axon defects, bind and bundle actin, bind Ca^{2+}, and whether actin-bundling activity is Ca^{2+} regulated.

examined were able to modulate the phenotype of *smn* morphant axons suggesting that PLS3 has unique properties that may be independent of actin binding. Even though other actin modifiers have been implicated to play roles in SMA (28,38,65,66), only PLS2 was able to compensate for PLS3 in this assay. Interestingly, PLS1, which also is able to bind and bundle actin filaments, could not rescue axon defects. A detailed analysis of PLS1's calcium sensitivity has not been determined and could lend insight into its inability to rescue. Alternatively, because PLS1 can bind and bundle actin, it also supports an actin-independent role for PLS3 in motor axons.

Though all of our data support an actin-independent role for PLS3 in motor axon outgrowth in *smn*-deficient neurons, we cannot eliminate the possibility that an interaction with actin plays some partial role for PLS3 in motor axon outgrowth of *smn* morphant embryos. Because we were unable to see a complete rescue of motor axons with the PLS3 construct lacking actin-binding domains (ΔABD1/2), it is possible that ΔABD1/2 is unable to fully compensate for full-length PLS3 function because it needs to associate with actin in some capacity. Increasing the dosage of ΔABD1/2 did not result in an increased ability to rescue axon defects, indicating that insufficient protein production was not to blame for a lack of complete phenotypic rescue. While ΔABD1/2 may be lacking some important sequence or domain necessary to function in a way comparable with full-length PLS3, this could also indicate that ΔABD1/2 conformation is compromised. Without full knowledge of the mechanism of PLS3 in motor axon outgrowth, it is not possible to distinguish between these possibilities.

While our work points toward an actin-independent role for PLS3, we further wanted to define how PLS3 interacted with actin and what role calcium played in this interaction. We examined the ability of full-length PLS3, the EF hand deletion (ΔEF hands) and the Ca^{2+}-binding mutant (EF mut 1 + 2) constructs to interact with actin filaments across a range of Ca^{2+} concentrations. Data from both a light scattering assay and a co-sedimentation assay conclusively demonstrated that PLS3 bundling activity of filamentous actin is negatively regulated by Ca^{2+}. These data were particularly intriguing as it only applied to PLS3 bundling and not binding to actin, which was not affected by calcium. In fact, actin filament stabilization by PLS3 was shown to be independent of Ca^{2+} concentration *in vitro* (36). However, another group had demonstrated that Ca^{2+} does exert tertiary structural changes to PLS3's EF hands (43) and actin-crosslinking by PLS3 has been demonstrated to be Ca^{2+} dependent (67). While we do demonstrate the ability of PLS3 actin-bundling function to be negatively regulated by Ca^{2+}, we cannot draw conclusions solely from these data in regard to *smn* morphant axon outgrowth. However, we convincingly demonstrate that both axon outgrowth and actin-bundling activity are regulated by Ca^{2+} interaction with PLS3. Because PLS3 constructs which retain the ability to bind and bundle actin filaments (ΔEF hands and EF mut 1 + 2) are unable to rescue *smn* morphant axons and PLS3 lacking actin-binding domains (ΔABD1/2) still retain ability to do so, our data in sum are in support of a role for PLS3 beyond solely that of interacting with actin.

Because our data define a novel Ca^{2+}-dependent function for PLS3 in *smn* morphant axon outgrowth, potential mechanisms for PLS3 function must meet these requirements. Several functions have been ascribed to PLS3 that could meet such qualifications. Because Ca^{2+} binding to the EF hands of PLS3 leads to conformational changes (43), it is possible that such structural changes could be important for PLS3 functions beyond interacting with actin. Furthermore, PLS2 is able to perform the same role as PLS3 in motor axons, while PLS1 cannot. In looking at reported functions of PLS2 and PLS3, both are reported to interact with Rab5 (57), a marker of early endosomes. While overexpression of PLS3 *in vitro* stimulated Rab5-mediated endocytosis, it has not been determined whether PLS3 is important for endocytosis *in vivo*. Interestingly, the yeast ortholog of PLS3, SAC6p, is required for endocytosis, as yeast deficient in SAC6p have abnormal morphology and defects in endocytosis (53,54). In addition, we have previously shown that PLS3 can rescue synaptic SV2 defects in *smn* mutant zebrafish (27). Furthermore, another infantile/juvenile onset motoneuron disorder, an atypical form of ALS, ALS2 is caused by mutations in alsin, a guanine nucleotide exchange factor for the small GTPase, Rab5 (68). Thus, disruptions to the endocytic pathway can lead to early onset motoneuron disease. Perhaps modulation of this pathway in SMA is ameliorated by the disease-modifying effect of PLS3. Indeed, PLS3 expression is able to restore synaptic vesicle number in NMJs in an SMA mouse model (29). In sum, these data suggest a potential role for PLS3 in synaptic vesicle endocytosis. Given that a genetic model of SMA in zebrafish also has neuromuscular junction defects (69) and that PLS3 expression is able to rescue these

observed defects (27), we would predict that PLS3 interaction with Rab5 may be an important mechanism to investigate in future work.

Since both PLS2 and PLS3 are able to rescue axon outgrowth phenotypes of *smn* morphant embryos, and both are known to be regulated by calcium, additional potential mechanisms can be proposed from knowledge of known PLS2-binding partners and function in signaling pathways. Interaction of PLS2 with grancalcin is regulated by calcium concentration (55). Additionally, PLS2 has been shown to interact with β-integrin (56), but it was not determined whether this interaction was calcium dependent. Also, ataxin2, the gene implicated in the polyglutamine expansion disorder spincerebellar ataxis 2, has been shown to co-immunoprecipitate with both PLS2 and PLS3 in mouse brain lysate (70). Intriguingly, ATX2, which has known roles in RNA metabolism (70–73) may also regulate PLS3 expression levels (70). ATX2 with the polyglutamine expansion caused strong cytoplasmic accumulation of PLS3 in mammalian cells (70). Furthermore, ATX2 also interacts with endophilin-A3 and A1 proteins, which have known roles in clathrin-mediated endocytosis (74–77). Investigation of these mechanisms of PLS2 interaction may lead further insight into the mode of action of PLS3 in motor axon outgrowth.

Understanding the mechanisms by which genetic modifiers modulate the course of SMA will be of importance in understanding the mechanisms of disease pathogenesis. While PLS3 is certainly not the only disease modifier, as it is not expressed by all discordant families (22,24) and different strains of SMA model mice display different disease time courses (29), it does seem to provide some protection in both humans and animal models of disease (22,27,29). Because other actin modifying proteins have been implicated to play roles in SMA (38,65) and homologs of both PLS3 (*plst-1*, Fim) and ACTN1 (*atn-1*, Actinin) were identified in modifier screens in invertebrates (28), we reasoned that PLS3 likely was modifying SMA phenotypes by modulating the actin cytoskeleton. We were surprised to discover that PLS3's role in SMA extends beyond that of modulation of actin, and that Ca^{2+} regulation of this process is necessary. Further investigation of PLS3's actin independent, Ca^{2+}-regulated function in motor axon outgrowth may lend insight into not only the mechanism of pathogenesis of SMA, but also motoneuron development in general.

MATERIALS AND METHODS

Zebrafish maintenance

Adult and larval zebrafish (*Danio rerio*) were maintained at The Ohio State University fish facility at 28.5°C and bred according to established procedures (78). Animal protocols were approved by the Ohio State University Committee on Use and Care of Animals.

Western blots

One-cell stage embryos were injected with RNA generated from different PLS3 constructs. At 10 and 24 hpf, 15 embryos from each injection were dechorionated, and resuspended in 45 μl homogenizing buffer (63 mM Tris pH 6.8, 5 mM EDTA, 10% SDS) with protease inhibitor cocktail. Tissue was boiled and centrifuged at 12 000*g* for 5 min at 4°C. Samples were added to 45 μl of 2× SDS sample buffer (100 mM Tris pH 6.8, 0.2% bromophenol blue, 20% glycerol, 200 mM dithiothreitol) and boiled for 5 min before loading to gels. For western blots 12 μl of protein lysates (equal to ∼2 embryos) were separated on 7.5 or 15% SDS–polyacrylamide gels depending on the size of the protein and transferred to polyvinylidene difluoride membranes (Immobilon P, Millipore). Blots were blocked for 1 h with 5% milk and 1% BSA in PBS with 0.1% Tween20 (PBST) and probed with mouse anti- β-actin (1:1000, C4, SantaCruz) and mouse anti-V5 (1:5000, Life Technologies) in 1% milk, 0.2% BSA/PBST overnight (ON) at 4°C. Following four washes with PBST for 5 min each, blots were incubated for 1 h at room temperature with the goat anti-mouse IgG-HRP, 1:5000 (Jackson ImmunoResearch Laboratories, Inc.) in 1% milk, 0.2% BSA/PBST. After five washes with PBST for 5 min each, signal was detected by chemiluminescence (Amersham Western Blotting Detection Reagents, GE Healthcare) on film. β-Actin was used as a protein loading control and was detected on the same western blots as the PLS3 forms after stripping and re-probing with the anti-β-actin antibody.

DNA constructs

Full-length human PLS3 cDNA (NCBI: NM_005032) in pcDNA3.1 was a gift from Brunhilde Wirth (22). Other clones information is as follows: Human cofilin-1 (NCBI: BC012265) ThermoScientific Bio (MGC 9272, human 3862540 pCMV-SPORT6.1); zebrafish profilin 2 (NCBI: BC067152.1) Life Technologies, (MGC: 77530, zebrafish 6702689 pCMV-SPORT6); human α-actinin 1 (NCBI: BC015766) ThermoScientificBio (MGC: 23191, human 4856734 pOTB7); human PLS1 (NCBI: BC031083.1) ATCC: MGC-33811 (human 5297758 pBluescriptR); human PLS2 (LCP1, L-plastin, NCBI: BC007673.1) ATCC: MGC-831 (human 3143290 pOTB7).

Amplification of PLS3, PLS3 deletions, human cofilin, zebrafish profilin-2 and human α-actinin1 was performed by PCR amplification of cDNA without the stop codon using primers as specified in Supplementary Material, Table S1. PCR products were cloned into pCR8/GW/TOPO vector according to manufacturer's directions (Life Technologies). Automated sequencing was performed to verify constructs. Directional cloning into pcDNA-DEST40, containing C-terminal V5 and 6xHis tags, was performed using LR Clonase II (Life Technologies). Mutagenesis of EF hand mutant clones was obtained by sequential mutagenesis of full-length PLS3 using the following primers: EF mut1-1 F 5′-AGGCCTTTGCAAAAGTTGC TCTCGCCAGCGCCGGATTCATTTGTGACT-3′, EF mut1-1 R 5′-AGTCACAAATGAATCCGGCGCTGGCGAGAGCAA CTTTTGCAAAGGCCT-3′, EF mut 1-2 F 5′-TCGCCAGCG CCGGAGCCATTGCTGACTATGCACTTCATGAGCTCT-T-3′, EF mut 1-2 R 5′-AAGAGCTCATGAAGTGCATAGTC AGCAATGGCTCCGGCGCTGGCGA-3′, EF mut 2-1 F 5′-ATGCTGGATGGTGCCAGGGCTAAAGCTGGGAAAATA-AGTTT-3′, EF mut 2-1 R 5′-AAACTTATTTTCCCAGCTT TAGCCCTGGCACCATCCAGCAT-3′, EF mut 2-2 F 5′-AG GGCTAAAGCTGGGGCAATAGCTTTTGACGCATTTGT-TTATATTTT-3′ and EF mut 2-2 R 5′-AAAATATAAACA AATGCGTCAAAAGCTATTGCCCCAGCTTTAGCCCT-3′. EF mut 1 was obtained by sequential reactions with EF mut 1-1

primers followed by mutagenesis with EF mut 1-2 primers using PLS3 pDEST40 as a template. EF mut 2 was obtained by sequential reactions with EF mut 2-1 primers followed by mutagenesis with EF mut 2-2 primers using PLS3 pDEST40 as a template. EF mut 1 + 2 was obtained by sequential reactions with EF mut 2-1 primers followed by mutagenesis with EF mut 2-2 primers using PLS3 EF mut 1 pDEST40 as a template. All reactions were carried out using the Stratagene QuikChange Site-Directed mutagenesis kit (Agilent Technologies) according to manufacturer's directions. All constructs were verified by sequencing (Plant-Microbe Genomics Facility, The Ohio State University).

Cell culture and transfections

HEK293 cells were grown in Dubecco's modification of Eagle's medium (Cellgro), supplemented with 10% fetal bovine serum (Cellgro) and 1% penicillin-streptomycin (Cellgro) at 37°C with 5% CO_2. HEK293 cells were seeded and plated at 1.0×10^6 cells/well in six-well plates 24 h preceding transfection. Cells were transfected with Lipofectamine 2000 (Life Technologies) according to manufacturer's directions in reduced serum media: 75% Opti-MEM I (Gibco), 25% cell culture growth media, (2.5% serum total); 4.0 μg of plasmid DNA was transfected; 24 h after transfection, cells were reseeded and plated on coverslips (ChemGlass Life Sciences LLC) in 24-well plates in quadruplicate; 24 h after cells were replated, they were fixed by drop-wise addition of 4% PFA directly to cell culture media.

mRNA transcription

PLS3 pcDNA3.1 vector and all pDEST40 vectors were linearized using AvrII. Full-length PLS3 synthetic capped mRNA from pcDNA3.1 was produced using the mMESSAGE mMACHINE T7 kit according to manufacturer's directions. All other synthetic capped mRNA from pCS2+ and pDEST40 were produced using the mMESSAGE mMACHINE SP6 kit. Capped mRNA was suspended in nuclease-free dH_2O and concentration was determined by spectrophotometry (Nanodrop 2000c, Thermo Scientific). Quality was checked by running 1 μl of RNA on a 2% agarose /SB (10 mM NaOH, H_3BO_3 to pH8.5) gel at 200 V for 15 min. Samples were stored at −80°C. Expression of V5-tagged constructs was verified by western blot at 28 hpf.

MO and RNA injections

smn translation blocking morpholino (5′-CGACATCTT CTGCACCATTGGC-3′) and a standard control morpholino (5′-CCTCTTACCTCAGTTACAATTTATA-3′) were synthesized (Gene-Tools, LLC) and injected at 1 nl/embryo into one to two cell stage Tg(*mnx1:0.6hsp70*:EGFP)os26 embryos as previously described (22,25). Stock MO solutions (2 mM) were prepared by resuspending the oligonucleotide in sterile filtered water heated to 65°C and aliquots were stored at RT. Each batch of *smn* MO was calibrated to produce ∼80% reduction of Smn protein. Under these conditions, the same range of defects is observed with the calibrated dose of *smn* MO, between 4.5 and 9.0 ng depending on batch efficacy. Working MO solutions (4–10 ng/nL) were prepared by dilution of 2 mM stock MO with sterile water containing 1% phenol red. Following injection, embryos were placed in filtered fish water with penicillin–streptomycin solution (Life Technologies) on a warm plate (28°C) to recover. Four hours following injections, embryos that did not contain phenol red in cells were discarded.

Motor axon scoring

At ∼28 hpf, embryos with normal morphology (∼80–90% of those injected) were fixed with 4% PFA for 24 h. The ventrally projecting caudal primary motoneurons were scored for morphological defects. Tg(*mnx1:0.6hsp70*:EGFP)os26 embryos strongly express EGFP in primary motor axons (79). Eight axons on each side of the embryo (16 total for each embryo) were scored for defects in morphology and classified as severe, moderate, mild or not defective. The classification of axons was utilized to give each fish an overall classification using criteria described in Supplementary Material, Table S2. Approximately 25 embryos per injection were scored for each condition with at least three injections per condition. Mann–Whitney analysis was performed to compare groups. Axons were imaged on a Zeiss axioplan microscope at ×40.

Immunofluorescence on cultured cells

Eight per cent PFA/PBS was gently added to culture media (4% final concentration of PFA) for 20 min to fix cells. Cells were washed twice with PBS and permeabilized with 0.1% TritonX-100/PBS (Fisher Scientific) for 10 min. Cells were washed twice with PBS. Immunofluorescent staining was performed in a humidity chamber (10-cm plate containing four pieces of wet paper towel covered by parafilm). Cells were placed cell-side down onto 35 μl solution: 1% BSA/PBS for 1 h, 1′ antibody (V5 antibody, 1:200 in 1% BSA/PBS, Life Technologies) for 1 h. Cells were washed twice with PBS and incubated in 2′ antibody (AlexaFluor 594 Rabbit Anti-Mouse IgG (H + L), 1:200 in 1% BSA/PBS, Life Technologies) for 40 min. Cells were washed twice with PBS and stained with AlexaFluor 488 phalloidin (1:40 in 1% BSA/PBS, Life Technologies) for 20 min. Cells were washed twice with PBS, vacuum-dried and mounted using DAPI-Fluoromount-G mounting medium (Southern Biotech). For each experiment, one of the quadruplicate replicates was not incubated in 1′ antibody to ensure that staining was not a result of non-specific binding of 2′ antibody. Cells were visualized using an Olympus Fluoview 1000 Laser Scanning Confocal microscope at ×60. Image stacks of 20 sections per cell were 10 μm in thickness in order to obtain the entire thickness of the cell. Image processing was performed with Photoshop 6.0.

Bacterial protein expression and purification

PLS3 full-length protein and its mutants (EF mut 1 + 2, ΔEF hands, and ΔABD1/2) were subcloned into pColdI vector (Takara) in-frame with the N-terminal 6xHis tag using the Infusion HD Enzyme cloning kit (Clontech). All proteins were expressed in Rosetta(DE3)pLysS *E. coli* strain (Novagen) at 15°C ON in the presence of 1 mM IPTG. Protein purification was carried out using HisPur Cobalt Resin (Thermo Scientific) according to the manufacturer's instructions. The expressed

proteins were stepwise eluted with 20, 50 and 250 mM imidazole and fractions containing uncontaminated proteins (>90% purity) revealed by SDS–PAGE analysis were pooled together and dialyzed against buffer containing 20 mM Tris, pH 8.0, 100 mM NaCl, 0.1 mM PMSF.

Actin preparation

Rabbit skeletal muscle actin was prepared from acetone powder (Pel-Freez Biologicals) as described in (80) and stored in G-buffer (5.0 mM Tris, pH 8.0, 0.2 mM Ca^{2+}-ATP, 5.0 mM β-mercaptoethanol). Before polymerization G-actin was treated with 0.1 mM $MgCl_2$ and 0.2 mM EGTA to exchange Ca^{2+} ions bound to actin to Mg^{2+}. G-actin was polymerized by adding $MgCl_2$ and KCl to final concentrations of 1 and 30 mM, respectively, and incubating for 1 h in the presence or absence of phalloidin at 4°C.

Light scattering measurement of actin bundle formation by PLS3

Light scattering analysis was performed at an angle of 90° to the incident light at the excitation and emission wavelengths set at 330 nm in a FlouroMax-3 spectrofluorometer (Jobin Yvon Horiba). Final concentrations of filamentous Mg^{2+}-F-actin and PLS3 proteins were 5 and 2 μM, respectively, in buffer A containing 20 mM Hepes, pH 7.5, 0.1 mM ATP, 1 mM DTT, 1 mM $MgCl_2$, 30 mM KCl, 0.1 mM EGTA.

Actin-binding and bundling sedimentation assays

About 5 μM of Mg^{2+}-F-actin and 2 μM of PLS3 or its mutants were mixed in buffer A supplemented with different concentrations of $CaCl_2$ to get the desired concentrations of free Ca^{2+} calculated using the Maxchelator software program for determining free metal concentrations (http://www.stanford.edu/~cpatton/CaMgATPEGTA-NIST-Plot.htm; last accessed on 30 November 2013). After ON incubation at 4°C, the samples were split and centrifuged either at high speed [200 000*g* for 30 min in TL-100 ultracentrifuge (Beckman)] to assess binding of PLS3 proteins to F-actin or at low speed (17 000*g* for 15 min) to estimate bundling abilities of these proteins. Supernatant and pellet fractions from both sedimentation assays were analyzed on SDS-polyacrylamide gels, stained with Coomassie Brilliant Blue, and quantified using the ImageJ software (Rasband, W.S., ImageJ, U. S. National Institutes of Health, Bethesda, MD, USA, http://imagej.nih.gov/ij/, 1997–2012, last accessed on 30 November 2013). Similar results were obtained using F-actin polymerized in the presence or absence of phalloidin.

SUPPLEMENTARY MATERIAL

Supplementary Material is available at *HMG* online.

ACKNOWLEDGEMENTS

We would like to thank the fish facility staff for their excellent fish care and facility maintenance.

Conflicts of Interest statement. None declared.

FUNDING

This work was supported by The National Institutes of Health [grant number R01NS050414] to C.E.B. with additional support from The OSU Neuroscience Center [grant number P30NS045758].

REFERENCES

1. Lefebvre, S., Burglen, L., Reboullet, S., Clermont, O., Burlet, P., Viollet, L., Bénichou, B., Cruaud, C., Millasseau, P. and Zeviani, M. (1995) Identification and characterization of a spinal muscular atrophy-determining gene. *Cell*, **80**, 155–165.
2. Roberts, D., Chavez, J. and Court, S. (1970) The Genetic Component in Child Mortality. *Arch. Dis. Child.*, **45**, 33.
3. Pearn, J. (1980) Classification of spinal muscular atrophies. *Lancet*, **1**, 919–922.
4. Melki, J., Lefebvre, S., Burglen, L., Burlet, P., Clermont, O., Millasseau, P., Reboullet, S., Bénichou, B., Zeviani, M. and Le Paslier, D. (1994) De novo and inherited deletions of the 5q13 region in spinal muscular atrophies. *Science*, **264**, 1474–1477.
5. McAndrew, P., Parsons, D., Simard, L., Rochette, C., Ray, P., Mendell, J., Prior, T. and Burghes, A. (1997) Identification of proximal spinal muscular atrophy carriers and patients by analysis of SMNT and SMNC gene copy number. *Am. J. Hum. Genet.*, **60**, 1411–1422.
6. Feldkötter, M., Schwarzer, V., Wirth, R., Wienker, T.F. and Wirth, B. (2002) Quantitative analyses of SMN1 and SMN2 based on real-time lightCycler PCR: fast and highly reliable carrier testing and prediction of severity of spinal muscular atrophy. *Am. J. Hum. Genet.*, **70**, 358–368.
7. Mailman, M.D., Heinz, J.W., Papp, A.C., Snyder, P.J., Sedra, M.S., Wirth, B., Burghes, A.H.M. and Prior, T.W. (2002) Molecular analysis of spinal muscular atrophy and modification of the phenotype by SMN2. *Genet. Med.*, **4**, 20–26.
8. Prior, T.W., Snyder, P.J., Rink, B.D., Pearl, D.K., Pyatt, R.E., Mihal, D.C., Conlan, T., Schmalz, B., Montgomery, L., Ziegler, K. *et al.* (2010) Newborn and carrier screening for spinal muscular atrophy. *Am. J. Med. Genet. A*, **152A**, 1608–1616.
9. Burghes, A.H.A. (1997) When is a deletion not a deletion? When it is converted. *Am. J. Hum. Genet.*, **61**, 9–15.
10. Lorson, C.L., Hahnen, E., Androphy, E.J. and Wirth, B. (1999) A single nucleotide in the SMN gene regulates splicing and is responsible for spinal muscular atrophy. *Proc. Natl Acad. Sci. USA*, **96**, 6307–6311.
11. Monani, U.R., Lorson, C.L., Parsons, D.W., Prior, T.W., Androphy, E.J., Burghes, A.H. and McPherson, J.D. (1999) A single nucleotide difference that alters splicing patterns distinguishes the SMA gene SMN1 from the copy gene SMN2. *Hum. Mol. Genet.*, **8**, 1177–1183.
12. Lorson, C.L. and Androphy, E.J. (2000) An exonic enhancer is required for inclusion of an essential exon in the SMA-determining gene SMN. *Hum. Mol. Genet.*, **9**, 259–265.
13. Cartegni, L. and Krainer, A.R. (2002) Disruption of an SF2/ASF-dependent exonic splicing enhancer in SMN2 causes spinal muscular atrophy in the absence of SMN1. *Nat. Genet.*, **30**, 377–384.
14. Kashima, T. and Manley, J.L. (2003) A negative element in SMN2 exon 7 inhibits splicing in spinal muscular atrophy. *Nat. Genet.*, **34**, 460–463.
15. Vitali, T., Sossi, V., Tiziano, F., Zappata, S., Giuli, A., Paravatou-Petsotas, M., Neri, G. and Brahe, C. (1999) Detection of the survival motor neuron (SMN) Genes by FISH: further evidence for a role for SMN2 in the modulation of disease severity in SMA patients. *Hum. Mol. Genet.*, **8**, 2525–2532.
16. Harada, Y., Sutomo, R., Sadewa, A.H., Akutsu, T., Takeshima, Y., Wada, H., Matsuo, M. and Nishio, H. (2002) Correlation between SMN2 copy number and clinical phenotype of spinal muscular atrophy: three SMN2 copies fail to rescue some patients from the disease severity. *J. Neurol.*, **249**, 1211–1219.
17. Prior, T.W., Krainer, A.R., Hua, Y., Swoboda, K.J., Snyder, P.C., Bridgeman, S.J., Burghes, A.H.M. and Kissel, J.T. (2009) A positive modifier of spinal muscular atrophy in the SMN2 Gene. *Am. J. Hum Genet.*, **85**, 408–413.

18. Rudnik-Schoneborn, S., Wirth, B. and Zerres, K. (1994) Evidence of autosomal dominant mutations in childhood-onset proximal spinal muscular atrophy. *Am. J. Hum. Genet.*, **55**, 112–119.
19. Capon, F. (1996) Discordant clinical outcome in type III spinal muscular atrophy sibships showing the same deletion pattern. *Neuromuscul. Disord.*, **6**, 261–264.
20. Helmken, C., Hofmann, Y., Schoenen, F., Oprea, G., Raschke, H., Rudnik-Schöneborn, S., Zerres, K. and Wirth, B. (2003) Evidence for a modifying pathway in SMA discordant families: reduced SMN level decreases the amount of its interacting partners and Htra2-beta1. *Hum. Genet.*, **114**, 11–21.
21. Prior, T.W., Swoboda, K.J., Scott, H.D. and Hejmanowski, A.Q. (2004) HomozygousSMN1 deletions in unaffected family members and modification of the phenotype bySMN2. *Am. J. Med. Genet.*, **130A**, 307–310.
22. Oprea, G.E., Kröber, S., McWhorter, M.L., Rossoll, W., Müller, S., Krawczak, M., Bassell, G.J., Beattie, C.E. and Wirth, B. (2008) Plastin 3 is a protective modifier of autosomal recessive spinal muscular atrophy. *Science*, **320**, 524–527.
23. Stratigopoulos, G., Lanzano, P., Deng, L., Guo, J., Kaufmann, P., Darras, B., Finkel, R., Tawil, R., McDermott, M.P., Martens, W. *et al.* (2010) Association of plastin 3 expression with disease severity in spinal muscular atrophy only in postpubertal females. *Arch. Neurol.*, **67**, 1252–1256.
24. Bernal, S., Also-Rallo, E., Martínez-Hernández, R., Alías, L., Rodríguez-Alvarez, F.J., Millán, J.M., Hernández-Chico, C., Baiget, M. and Tizzano, E.F. (2011) Plastin 3 expression in discordant spinal muscular atrophy (SMA) siblings. *Neuromuscul. Disord.*, **21**, 413–419.
25. McWhorter, M.L., Monani, U.R., Burghes, A.H.M. and Beattie, C.E. (2003) Knockdown of the survival motor neuron (Smn) protein in zebrafish causes defects in motor axon outgrowth and pathfinding. *J. Cell Biol.*, **162**, 919–931.
26. Hao, L.T., Duy, P.Q., Jontes, J.D., Wolman, M., Granato, M. and Beattie, C.E. (2013) Temporal requirement for SMN in motoneuron development. *Hum. Mol. Genet.*, **22**, 2612–2625.
27. Hao, L.T., Wolman, M., Granato, M. and Beattie, C.E. (2012) Survival motor neuron affects plastin 3 protein levels leading to motor defects. *J. Neurosci.*, **32**, 5074–5084.
28. Dimitriadi, M., Sleigh, J.N., Walker, A., Chang, H.C., Sen, A., Kalloo, G., Harris, J., Barsby, T., Walsh, M.B., Satterlee, J.S. *et al.* (2010) Conserved genes act as modifiers of invertebrate SMN loss of function defects. *PLoS Genet.*, **6**, e1001172.
29. Ackermann, B., Kröber, S., Torres-Benito, L., Borgmann, A., Peters, M., Hosseini Barkooie, S.M., Tejero, R., Jakubik, M., Schreml, J., Milbradt, J. *et al.* (2013) Plastin 3 ameliorates spinal muscular atrophy via delayed axon pruning and improves neuromuscular junction functionality. *Hum. Mol. Genet.*, **22**, 1328–1347.
30. Lin, C.S., Shen, W., Chen, Z.P., Tu, Y.H. and Matsudaira, P. (1994) Identification of I-plastin, a human fimbrin isoform expressed in intestine and kidney. *Mol. Cell Biol.*, **14**, 2457–2467.
31. Goldstein, D., Djeu, J., Latter, G., Burbeck, S. and Leavitt, J. (1985) Abundant synthesis of the transformation-induced protein of neoplastic human fibroblasts, plastin, in normal lymphocytes. *Cancer Res.*, **45**, 5643.
32. Lin, C.S., Aebersold, R.H., Kent, S.B., Varma, M. and Leavitt, J. (1988) Molecular cloning and characterization of plastin, a human leukocyte protein expressed in transformed human fibroblasts. *Mol. Cell Biol.*, **8**, 4659–4668.
33. Lin, C.S., Park, T., Chen, Z.P. and Leavitt, J. (2001) Human plastin genes. Comparative gene structure, chromosome location, and differential expression in normal and neoplastic cells. *J. Biol. Chem.*, **268**, 2781–2792.
34. de Arruda, M.V., Watson, S., Lin, C.S., Leavitt, J. and Matsudaira, P. (1990) Fimbrin is a homologue of the cytoplasmic phosphoprotein plastin and has domains homologous with calmodulin and actin gelation proteins. *J. Cell Biol.*, **111**, 1069–1079.
35. Volkmann, N., DeRosier, D., Matsudaira, P. and Hanein, D. (2001) An atomic model of actin filaments cross-linked by fimbrin and its implications for bundle assembly and function. *J. Cell Biol.*, **153**, 947–956.
36. Giganti, A., Plastino, J., Janji, B., Van Troys, M., Lentz, D., Ampe, C., Sykes, C. and Friederich, E. (2005) Actin-filament cross-linking protein T-plastin increases Arp2/3-mediated actin-based movement. *J. Cell Sci.*, **118**, 1255–1265.
37. Bernstein, B.W. and Bamburg, J.R. (2010) ADF/Cofilin: a functional node in cell biology. *Trends Cell Biol.*, **20**, 187–195.
38. Bowerman, M., Anderson, C.L., Beauvais, A., Boyl, P.P., Witke, W. and Kothary, R. (2009) SMN, profilin IIa and plastin 3: a link between the deregulation of actin dynamics and SMA pathogenesis. *Mol. Cell Neurosci.*, **42**, 66–74.
39. Birbach, A. (2008) Profilin, a multi-modal regulator of neuronal plasticity. *BioEssays*, **30**, 994–1002.
40. Sjöblom, B., Salmazo, A. and Djinović-Carugo, K. (2008) Alpha-actinin structure and regulation. *Cell Mol. Life Sci.*, **65**, 2688–2701.
41. Arpin, M., Friederich, E., Algrain, M., Vernel, F. and Louvard, D. (1994) Functional differences between L- and T-plastin isoforms. *J. Cell Biol.*, **127**, 1995–2008.
42. Adams, A.E., Shen, W., Lin, C.S., Leavitt, J. and Matsudaira, P. (1995) Isoform-specific complementation of the yeast sac6 null mutation by human fimbrin. *Mol. Cell Biol.*, **15**, 69–75.
43. Miyakawa, T., Shinomiya, H., Yumoto, F., Miyauchi, Y., Tanaka, H., Ojima, T., Kato, Y.S. and Tanokura, M. (2012) Different Ca^{2}?-sensitivities between the EF-hands of T- and L-plastins. *Biochem. Biophys. Res. Commun.*, **429**, 137–141.
44. Correia, I., Chu, D., Chou, Y.H., Goldman, R.D. and Matsudaira, P. (1999) Integrating the actin and vimentin cytoskeletons. adhesion-dependent formation of fimbrin-vimentin complexes in macrophages. *J. Cell Biol.*, **146**, 831–842.
45. Lin, C.S., Lau, A. and Lue, T.F. (1998) Analysis and mapping of plastin phosphorylation. *DNA Cell Biol.*, **17**, 1041–1046.
46. Janji, B., Giganti, A., De Corte, V., Catillon, M., Bruyneel, E., Lentz, D., Plastino, J., Gettemans, J. and Friederich, E. (2006) Phosphorylation on Ser5 increases the F-actin-binding activity of L-plastin and promotes its targeting to sites of actin assembly in cells. *J. Cell Sci.*, **119**, 1947–1960.
47. Delanote, V., Van Impe, K., De Corte, V., Bruyneel, E., Vetter, G., Boucherie, C., Mareel, M., Vandekerckhove, J., Friederich, E. and Gettemans, J. (2005) Molecular basis for dissimilar nuclear trafficking of the actin-bundling protein isoforms T- and L-plastin. *Traffic*, **6**, 335–345.
48. Kretsinger, R.H. and Nockolds, C.E. (1973) Carp muscle calcium-binding protein. II. Structure determination and general description. *J. Biol. Chem.*, **248**, 3313–3326.
49. Ikeda, H., Sasaki, Y., Kobayashi, T., Suzuki, H., Mita, H., Toyota, M., Itoh, F., Shinomura, Y., Tokino, T. and Imai, K. (2005) The role of T-fimbrin in the response to DNA damage: silencing of T-fimbrin by small interfering RNA sensitizes human liver cancer cells to DNA-damaging agents. *Int. J. Oncol.*, **27**, 933–940.
50. Delanote, V., Vandekerckhove, J. and Gettemans, J. (2005) Plastins: versatile modulators of actin organization in (patho)physiological cellular processes. *Acta. Pharmacol. Sin.*, **26**, 769–779.
51. Witke, W., Hofmann, A., Köppel, B., Schleicher, M. and Noegel, A.A. (1993) The Ca(2+)-binding domains in non-muscle type alpha-actinin: biochemical and genetic analysis. *J. Cell Biol.*, **121**, 599–606.
52. Glenney, J.R., Kaulfus, P., Matsudaira, P. and Weber, K. (1981) F-actin binding and bundling properties of fimbrin, a major cytoskeletal protein of microvillus core filaments. *J. Biol. Chem.*, **256**, 9283–9288.
53. E Kübler, H.R. (1993) Actin and fimbrin are required for the internalization step of endocytosis in yeast. *EMBO J.*, **12**, 2855.
54. Adams, A.E., Botstein, D. and Drubin, D.G. (1989) A yeast actin-binding protein is encoded by SAC6, a gene found by suppression of an actin mutation. *Science*, **243**, 231–233.
55. Lollike, K., Johnsen, A.H., Durussel, I., Borregaard, N. and Cox, J.A. (2001) Biochemical characterization of the penta-EF-hand protein grancalcin and identification of L-plastin as a binding partner. *J. Biol. Chem.*, **276**, 17762–17769.
56. Le Goff, E., Vallentin, A., Harmand, P.-O., Aldrian-Herrada, G., Rebière, B., Roy, C., Benyamin, Y. and Lebart, M.C. (2010) Characterization of L-plastin interaction with beta integrin and its regulation by micro-calpain. *Cytoskeleton (Hoboken)*, **67**, 286–296.
57. Hagiwara, M., Shinomiya, H., Kashihara, M., Kobayashi, K.-I., Tadokoro, T. and Yamamoto, Y. (2011) Interaction of activated Rab5 with actin-bundling proteins, L- and T-plastin and its relevance to endocytic functions in mammalian cells. *Biochem. Biophys. Res. Commun.*, **407**, 615–619.
58. Kong, L., Wang, X., Choe, D.W., Polley, M., Burnett, B.G., Bosch-Marcé, M., Griffin, J.W., Rich, M.M. and Sumner, C.J. (2009) Impaired Synaptic Vesicle Release and Immaturity of Neuromuscular Junctions in Spinal Muscular Atrophy Mice. *J. Neurosci.*, **29**, 842–851.

59. Ruiz, R., Casañas, J.J., Torres-Benito, L., Cano, R. and Tabares, L. (2010) Altered intracellular Ca2+ homeostasis in nerve terminals of severe spinal muscular atrophy mice. *J. Neurosci.*, **30**, 849–857.
60. Jablonka, S., Beck, M., Lechner, B.D., Mayer, C. and Sendtner, M. (2007) Defective Ca2+ channel clustering in axon terminals disturbs excitability in motoneurons in spinal muscular atrophy. *J. Cell Biol.*, **179**, 139–149.
61. McGivern, J.V., Patitucci, T.N., Nord, J.A., Barabas, M.-E.A., Stucky, C.L. and Ebert, A.D. (2013) Spinal muscular atrophy astrocytes exhibit abnormal calcium regulation and reduced growth factor production. *Glia*, **61**, 1418–1428.
62. Gomez, T.M. and Zheng, J.Q. (2006) The molecular basis for calcium-dependent axon pathfinding. *Nat. Rev. Neurosci.*, **7**, 115–125.
63. Namba, Y., Ito, M., Zu, Y., Shigesada, K. and Maruyama, K. (1992) Human T cell L-plastin bundles actin filaments in a calcium dependent manner. *J Biochem.*, **112**, 503–507.
64. Cingolani, L.A. and Goda, Y. (2008) Actin in action: the interplay between the actin cytoskeleton and synaptic efficacy. *Nat. Rev. Neurosci.*, **9**, 344–356.
65. Bowerman, M., Beauvais, A., Anderson, C.L. and Kothary, R. (2010) Rho-kinase inactivation prolongs survival of an intermediate SMA mouse model. *Hum. Mol. Genet.*, **19**, 1468–1478.
66. Nölle, A., Zeug, A., van Bergeijk, J., Tönges, L., Gerhard, R., Brinkmann, H., Rayes, Al, S., Hensel, N., Schill, Y., Apkhazava, D. *et al.* (2011) The spinal muscular atrophy disease protein SMN is linked to the Rho-kinase pathway via profilin. *Hum. Mol. Genet.*, **20**, 4865–4878.
67. Kovar, D.R., Staiger, C.J., Weaver, E.A. and McCurdy, D.W. (2000) AtFim1 is an actin filament crosslinking protein from *Arabidopsis thaliana*. *Plant J.*, **24**, 625–636.
68. Yang, Y., Hentati, A., Deng, H.X., Dabbagh, O., Sasaki, T., Hirano, M., Hung, W.Y., Ouahchi, K., Yan, J., Azim, A.C. *et al.* (2001) The gene encoding alsin, a protein with three guanine-nucleotide exchange factor domains, is mutated in a form of recessive amyotrophic lateral sclerosis. *Nat. Genet.*, **29**, 160–165.
69. Boon, K.-L., Xiao, S., McWhorter, M.L., Donn, T., Wolf-Saxon, E., Bohnsack, M.T., Moens, C.B. and Beattie, C.E. (2009) Zebrafish survival motor neuron mutants exhibit presynaptic neuromuscular junction defects. *Hum. Mol. Genet.*, **18**, 3615–3625.
70. Ralser, M., Nonhoff, U., Albrecht, M., Lengauer, T., Wanker, E.E., Lehrach, H. and Krobitsch, S. (2005) Ataxin-2 and huntingtin interact with endophilin-A complexes to function in plastin-associated pathways. *Hum. Mol. Genet.*, **14**, 2893–2909.
71. Shibata, H., Huynh, D.P. and Pulst, S.M. (2000) A novel protein with RNA-binding motifs interacts with ataxin-2. *Hum. Mol. Genet.*, **9**, 1303–1313.
72. Kedersha, N., Cho, M.R., Li, W., Yacono, P.W., Chen, S., Gilks, N., Golan, D.E. and Anderson, P. (2000) Dynamic shuttling of TIA-1 accompanies the recruitment of mRNA to mammalian stress granules. *J. Cell Biol.*, **151**, 1257–1268.
73. Kedersha, N. and Anderson, P. (2002) Stress granules: sites of mRNA triage that regulate mRNA stability and translatability. *Biochem. Soc. Trans.*, **30**, 963–969.
74. de Heuvel, E., Bell, A.W., Ramjaun, A.R., Wong, K., Sossin, W.S. and McPherson, P.S. (1997) Identification of the major synaptojanin-binding proteins in brain. *J. Biol. Chem.*, **272**, 8710–8716.
75. Soubeyran, P., Kowanetz, K., Szymkiewicz, I., Langdon, W.Y. and Dikic, I. (2002) Cbl-CIN85-endophilin complex mediates ligand-induced downregulation of EGF receptors. *Nature*, **416**, 183–187.
76. Nonis, D., Schmidt, M.H.H., van de Loo, S., Eich, F., Dikic, I., Nowock, J. and Auburger, G. (2008) Ataxin-2 associates with the endocytosis complex and affects EGF receptor trafficking. *Cell Signal.*, **20**, 1725–1739.
77. Ung, C.Y., Li, H., Ma, X.H., Jia, J., Li, B.W., Low, B.C. and Chen, Y.Z. (2008) Simulation of the regulation of EGFRendocytosis and EGFR-ERK signaling by endophilin-mediated RhoA-EGFR crosstalk. *FEBS Lett.*, **582**, 2283–2290.
78. Westerfield, M. (2000) *The Zebrafish Book*, 4th edn. Univ. of Oregon Press, Eugene, OR.
79. Dalgin, G., Ward, A.B., Hao, L.T., Beattie, C.E., Nechiporuk, A. and Prince, V.E. (2011) Zebrafish mnx1 controls cell fate choice in the developing endocrine pancreas. *Development*, **138**, 4597–4608.
80. Spudich, J.A. and Watt, S. (1971) The regulation of rabbit skeletal muscle contraction. I. Biochemical studies of the interaction of the tropomyosin-troponin complex with actin and the proteolytic fragments of myosin. *J. Biol. Chem.*, **246**, 4866–4871.